3-D Deployment and Trajectory Planning for Relay Based UAV Assisted Cooperative Communication for Emergency Scenarios Using Dijkstra's Algorithm

Nelapati Lava Prasad, *Graduate Student Member, IEEE*, and Barathram Ramkumar

***Abstract*—In this work, a relay-based UAV-assisted cooperative communication for emergency applications is proposed for rural and semi-urban scenarios. 3-D deployment of multiple UAVs is resolved by jointly optimizing the height and transmit power of cluster UAVs and the optimal trajectory of relay UAVs is perfected by using the graph theory approach. While the majority of works in literature use UAVs as aerial base stations or as relays, this paper proposes to use UAVs as both relays and aerial base stations. Furthermore, this is one of the few works where UAVs are used as both static base stations (cluster UAVs) and mobile base stations (relay UAVs). The proposed 3-D deployment and trajectory planning algorithm is implemented at the ground base station (GBS) and the resultant parameters will be distributed to cluster UAVs either directly or through relay UAVs. A four-step approach is proposed to solve the 2-D location coordinates of cluster UAVs, to find the location of the GBS, the power-height optimization of cluster UAVs, and to optimize the trajectory of relay UAVs. The number of users served, channel capacity achieved, power saved due to optimal deployment, latency reduced, and power saving by optimal trajectory are some of the performance metrics used to evaluate the proposed algorithms. The simulation results are validated to show that the proposed solutions outperform existing similar approaches.**

***Index Terms*—Unmanned Aerial Vehicles (UAV), cooperative communication, 3-D deployment, relay UAV, graph theory.**

I. Introduction

UNMANNED aerial vehicle (UAV) based wireless communication brings out huge attention of researchers and industries lately owing to their vast advantages over conventional wireless cellular communication. Due to their low cost, quick deployment, ubiquitous coverage, high maneuverability, and pliable changeability capabilities, UAV-based base stations (UAV-BSs) have innumerable applications in both commercial and military fields [1], [2], [3], [4], [5], [6]. Based on whether the flexible mobility of UAVs is utilized or not, they can be classified into static UAV-BS or mobile UAV-BS. UAVs can be used for various applications in different ways. The advantages of cooperative communication in a wireless environment are invaluable [6]. An aerial UAV-BS can be seen as a part of a robust, fast, and competent emergency communication system enabling effective communication of public safety information during natural disasters or temporary public events. In 2017, popular cellular service provider AT&T developed an LTE cell site mounted on a helicopter to provide a network after hurricane 'Maria' devastated the conventional ground network of all service providers in Puerto Rico [7]. The inspiration for this act is of course from the innovative projects of major organizations including Google's Project Loon [8], NASA's Pathfinder [9] under Environmental Research Aircraft and Sensor Technology program (ERAST), AeroVironment's Helios Prototype [10].

After emergencies such as earthquakes or cyclones where the existing ground cellular network is destroyed partially or fully, to provide wireless cellular service, one can deploy single or multiple UAV-BSs depending on the size of the area. Even though numerous applications are possible, deploying UAV-BSs is not simple but challenging and various issues have to be addressed. Since UAV power on board is limited and valuable, effective utilization of power for both flight and transmitting information is a must. Also, 3-D deployment is a potential challenge that got a great deal of attention lately.

A. Related Work

In recent years, many researchers worked on similar challenges. A detailed review of UAV-assisted wireless networks with their applications and challenges are listed in [3]. A single UAV-based aerial base station challenges were analyzed in [11], [12], [13], [14], [15], [16], [17], [18]. In [11], a single UAV is used as a relay for throughput maximization by jointly optimizing the transmit power and trajectory of UAV with well-known source and destination locations and by keeping height constant. Similar work is presented in [12], where a single UAV's height is kept constant and horizontal movement of UAV is optimized for throughput maximization. In [13], trajectory of single UAV is optimized to collect the data from the multiple ground sensor nodes. The work in [14] proposed that a single UAV is used as an aerial mobile relay where its transmission capability is powered by a radio signal sent from the ground source via the

Manuscript received 14 May 2022; revised 24 August 2022; accepted 15 November 2022. Date of publication 23 November 2022; date of current version 18 April 2023. This work was supported in part by the Visvesvaraya Ph.D.Scheme under Grant PhD-MLA/4(88)/2015-16, in part by MeitY, Government of India, in part by Impacting Research, Innovation and Technology (IMPRINT)-2 under Project IMP/2018/001719, and in part by the MHRD, Government of India through Scheme for Promotion of Academic and Research Collaboration (SPARC). The review of this article was coordinated by Dr. Lin X Cai. *(Corresponding author: Nelapati Lava Prasad.)*

The authors are with the School of Electrical Sciences, Indian Institute of Technology Bhubaneswar, Odisha 752050, India (e-mail: nlp10@iitbbs.ac.in; barathram@iitbbs.ac.in).

Digital Object Identifier 10.1109/TVT.2022.3224304

power splitting scheme. The authors in [15] proposed to use self-interference energy harvesting (SI-EH) technique along with simultaneous wireless information and power transfer (SWIPT) to improve single UAVs performance as relay between terrestrial base station and ground user. Similar to [14], the authors in [16] proposed a UAV-assisted cooperative communication based on SWIPT where a single UAV serves as a relay, and its transmission capability is powered by a radio signal received from the source via the time-sharing mechanism. In [17], a single UAV is used as a relay between source and destination of a device-to-device (D2D) communication for critical situations during post-disaster management. The authors in [18] aimed to provide a line of sight (LoS) connection to the cell edge nodes by optimizing the altitude of a single UAV as a relay where users with NLOS connection are assumed to be within the coverage range of conventional ground base station.

The work in [19] presented a downlink coverage probability of UAVs as a function of altitude by deploying multiple UAVs based on the circle packing method to maximize the total coverage area with a minimum number of UAVs used. In [20], a polynomial-time spiral algorithm is proposed to find the minimum number of UAVs required to provide coverage for a group of users. The condition here is that all the users are within the coverage range of at least one UAV which is practically difficult to get by in rural and semi-urban scenarios. The authors in [21] intended to use a minimum number of UAV-BSs to effectively cover a geographical area by optimizing multi-user communication scheduling & association, UAVs trajectory. The work in [22] aimed to determine the minimum number of UAVs required to cover a geographical area using a sparse recovery algorithm. Although in [22], UAVs considered are low altitude platform (LAP) drones that can only serve a few users. In [23], gravity-inspired clustering algorithm (GICA) is used to determine the 3D placement of multiple UAVs using ad-hoc approach to cover the non-uniformly distributed user equipment.

The concept of using UAVs to relay information between two nodes is considered in [24], [25], [26] in which case trajectory optimization plays a crucial role. The authors in [24] focused on trajectory optimization of rotary-wing UAVs which acts like a transceiver to communicate with multiple ground nodes by moving closer to each node via stop and collect mechanism. similarly, in [25], multiple UAVs are used as data collection devices in an IoT application where multiple IoT devices are present. The trajectory of multiple UAVs is optimized here to increase the data collection rate off UAVs where IoT devices' data transmission capability is powered by UAV's wireless power transfer method. In [26], an ultra-dense UAV-enabled wireless network is formed for cache data transmission where massive UAVs are deployed to transmit cached contents to a group of randomly distributed ground nodes.

B. Contribution of Paper

The majority of works in literature which use multiple UAVs considered the homogeneous scenario where UAVs are of the same functionality (either aerial base station or relay). In an emergency scenario, it is better to use heterogeneous UAVs where some act as aerial base stations and others as relays so that vast and inaccessible areas can be covered.

The authors of this paper, in their previous work [27], proposed a heterogeneous solution where the users distributed in a large area are grouped into clusters and each cluster is served by one cluster UAV and one relay UAV. The cluster UAV hovers at an optimal height and acts as an aerial base station and relay UAV transport information between a central server and cluster UAVs. The drawback of work in [27] is that more relay UAVs are required and the trajectory planning proposed for relay UAVs is not optimized and expensive. The drawbacks of [27] are addressed in this work where a modified heterogeneous solution is proposed to reduce the number of relay UAVs and optimize their trajectory. The main contributions of this work are outlined below:

1) In this work, a 3-D deployment, height-transmit power optimization, and trajectory optimization of multiple UAV-assisted cooperative communication is proposed for an emergency, temporary, or critical situations using cluster UAVs and relay UAVs.
2) The horizontal location coordinates of cluster UAVs are found using K-Medoids clustering algorithm and the performance is compared with other clustering algorithms such as K-Means, GICA, and uniform. Since K-Medoids clustering algorithm is more feasible than others owing to the minimum dissimilarity of cluster centroid with cluster users, the same is used to find the location of the ground base station (GBS).
3) An optimization problem is defined to find the optimal height and optimal transmit power of each cluster UAV and solve it for the effective utilization of available limited resources until a reliable solution is achieved.
4) A graph theory-based routing algorithm is used to find the optimized trajectory and the start & stop locations of relay UAVs. Since the travel cost of UAVs is more than the communication cost [13], the travel distance of relay UAVs is optimized, and cost and latency are reduced.
5) The adaptability and robustness of the proposed method are analyzed, the effect of various parameters under various situations is studied, and is found to be improved by using the proposed method compared to a few others in the literature.

The rest of the paper is organized as follows. In Section II, the system model and problem formulation are presented. Also, a scenario of a free space propagation model with LoS connection for cluster communication is drafted. The proposed 3-D deployment method along with height-power optimization is detailed in Section III. In Section IV, trajectory optimization of relay UAVs is solved. Simulation results are discussed in Section V followed by a conclusion in Section VI.

II. System Model and Problem Statement

The scenario considered in this paper is illustrated in Fig. 1. It is assumed that the users are distributed in a vast area and are typically distributed as clusters. This type of scenario is common

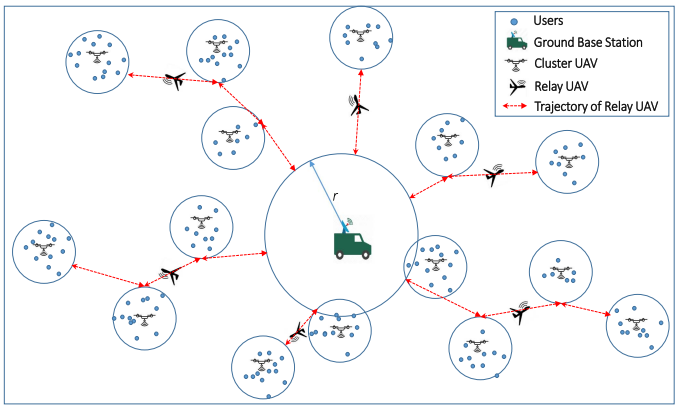

Fig. 1. Model of UAV assisted Cooperative Communication for Emergency Scenarios using cluster UAV, relay UAV, and ground base station (GBS).

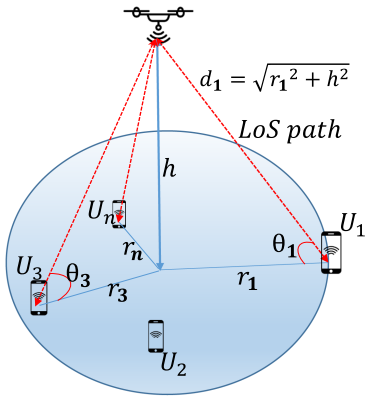

Fig. 2. Free space propagation model with LoS connection.

in mountainous regions where the population is clustered in valleys. This also models a rural scenario where villages are located amidst large agricultural fields. During emergencies like floods, cyclones, or landslides, these population clusters become isolated.

In this paper, the population size in a geographical area is taken as 'N'. The population is grouped into 'K' clusters with 'M' users in each cluster ($K * M = N$) which models the scenario in Fig. 1. The population distribution in the geographical area is modeled as a 2-D Gaussian mixture model with 'K' mixtures with mixing probability, mean, and variance as inputs. For 'K' clusters, UAV_{C_i}, $(i = 1, \ldots, K)$ are cluster UAVs and UAV_{R_i} $(i = 1, \ldots, L)$ are relay UAVs with $L \leq K$. For better communication, GBS is used only to serve UAVs, not users. It is assumed that all ground users are having similar transceiver characteristics. Also, the cluster UAVs serving the neighboring clusters are assumed to be operating at different central frequencies which will minimize the inter-UAV interference. For the communication between cluster UAV and its users, two different channel models are considered for analysis and are as follows:

A. Case 1: Free Space Propagation Model

The free space propagation model with LoS connection is illustrated in Fig. 2. Therefore the relation between power transmitted and received in LoS path with the free-space path loss model is given by [16]

$$P_r(i) = \frac{P_t}{(d_i)^{\alpha}}, \quad where \;\; d_i = \sqrt{(r_i)^2 + (h)^2} \tag{1}$$

where P_t is the power transmitted by the UAV, $P_r(i)$ is the power received by i^{th} user, d_i is the distance between i^{th} user and cluster UAV, h is the height of UAV, r_i is the horizontal distance between i^{th} user and cluster centre, and α is the path-loss exponent which depends on various environmental parameters [28]. For the rural and semi-urban scenarios, α for free space propagation is taken as 2 [28].

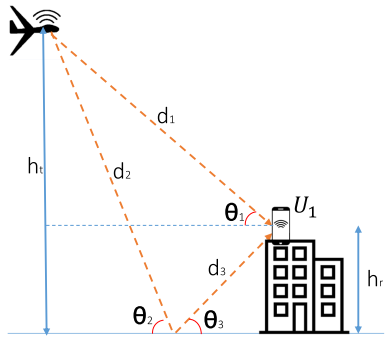

Fig. 3. Two-ray ground reflection model.

B. Case 2: Two-Ray Ground Reflection Model

The Two-ray ground reflection model with LoS & NLoS paths are illustrated in Fig. 3. Therefore the relation between power transmitted and received here is given by [28]

$$P_r(i) \propto \frac{P_t}{(d_i)^4}, \quad where \;\; d_i = \frac{\sqrt{h_t h_{ri}}}{\lambda} \tag{2}$$

where P_t is the power transmitted by the UAV, h_t is the transmitter height, h_{ri} is the height of the i^{th} user, and $P_r(i)$ is the power received by i^{th} user. It is to be noted that the proportionality in (2) also depends on antenna gains of the transmitter (G_t) and receiver (G_r).

The channel capacity for the i^{th} user can be derived from the Shannon capacity theorem and is taken as [28]

$$C(i) = W * log_2\left(1 + \frac{P_t/(d_i)^{\alpha}}{N_0(i) + I}\right) \; where \; I = \sum_{j=1}^{n} P_r(ij) \tag{3}$$

where W is the bandwidth of the channel, P_t is the power transmitted by the cluster UAV, and $N_0(i)$ is the noise power received by the i^{th} user. For free space LoS model, α is taken as 2 and d_i is computed using (1). For the hybrid LoS and NLoS model, α is taken as 4 and d_i is computed using (2). Here I is the co-channel interference from the neighboring UAVs, n is the number of co-channel UAVs, $P_r(ij)$ is the power received by the i^{th} user from the j^{th} co-channel UAV. Here $P_r(ij)$ can be calculated using (1) or (2) depending on the channel model considered.

The coverage area of i^{th} cluster UAV when communicating with ground users is modeled as a cone projection onto the

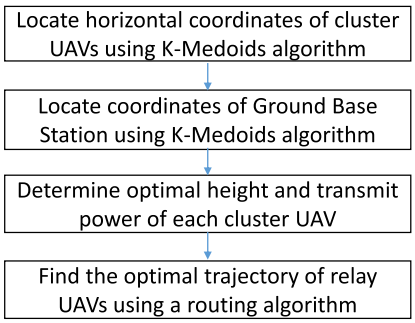

Fig. 4. Flowchart of the proposed approach.

ground with a coverage radius of 'r_{ci}'. Multiple access techniques are used to serve the users inside the clusters. The required bandwidth resources are assumed to be available.

As mentioned earlier, the objective of the paper is to provide wireless coverage to users distributed over a large area using multiple heterogeneous UAVs at an optimal cost and maintaining the quality of service (QoS). QoS in emergency scenarios includes network coverage to all users and cost factor includes optimal communication power and UAV travel cost. As illustrated in Fig. 1, it is assumed that at least one GBS is available. This can be a mobile base station mounted on a truck/vehicle with a satellite link. The location of the GBS can be anywhere in the area and need not be at the center.

The UAVs used here are classified into two types: cluster UAVs and relay UAVs. Cluster UAVs are used to serve the users in the clusters (groups). Once the horizontal coordinates of cluster UAVs are determined using unsupervised learning algorithms, then cluster UAVs only move in a vertical direction based on the optimal height given by the optimization problem. Relay UAVs are used to relay the information between GBS and cluster UAV if that cluster UAV is outside the coverage area of GBS. Rotary-wing UAVs are used as cluster UAVs which enables them to hover on top of cluster centroids at the desired height. This makes the cluster UAVs as static UAV-BS whereas relay UAVs can be treated as mobile UAV-BS as they travel to and fro through optimized trajectories. Hence fixed-wing UAVs can be used as relay UAVs which can fly for a longer duration and can carry a high payload. The proposed algorithm assumes that the knowledge of the population distribution of the area is available at the GBS. Usually, such data can be obtained from the cellular service providers operating in that area before the disaster. Based on that information and available resources (such as number of UAVs, battery capacity of UAVs, frequency spectrum availability, etc.), the proposed algorithm will be run on GBS and the resultant parameters will be distributed to cluster UAVs either directly (if cluster UAVs are within the coverage range of GBS) or through relay UAVs. To achieve the QoS, an optimal 3-D deployment and trajectory planning is proposed for a relay-based UAV-assisted cooperative communication using optimization and routing algorithm tools for emergency scenarios.

A four-step approach is proposed in this work as illustrated in Fig. 4. The first step is to find the horizontal location coordinates of cluster UAVs using unsupervised learning algorithms. The second step is to find the location of GBS based on the horizontal locations of cluster UAVs. In the third step, an optimization problem is defined to find the optimal height and optimal transmit power of each cluster UAV. In the final step, a graph theory approach is used to optimize the trajectory of relay UAVs.

Algorithm 1: Horizontal Locations of Cluster UAVs Using K-Medoids Algorithm.

1: Find distance matrix D for all N users using (5).
2: Find the dissimilarity index V_j for $j = 1$ to N using (4).
3: Arrange V_j in ascending order and choose first K smallest values (users) as initial cluster centroids.
4: **for** $i = 1$ to K (for each cluster) **do**
5: Sort $D(i, j)$ for for $j = 1$ to N in ascending order and assign first M users to cluster i
6: **end for**
7: **for** $i = 1$ to K (for each cluster) **do**
8: Find the sum of distances $D(i, l)$ for $l = 1$ to M users in i^{th} cluster
9: **for** $j = 1$ to $M - 1$ (within each cluster excluding the present centroid) **do**
10: Find the sum of distances $D(j, l)$ for $l = 1$ to M users in i^{th} cluster
11: **if** $D(j, l) < D(i, l)$ **then**
12: replace user i with user j as centroid, terminate inner for loop, and go back to step 8 with updated centroid i.
13: **end if**
14: **end for**
15: **end for**
16: Output (X_{ci}, Y_{ci}) for $i = 1$ to K as the horizontal location coordinates of cluster UAVs and corresponding M users of each cluster.

III. 3-D Deployment of Cluster UAVs

A. Horizontal Locations of Cluster UAVs (X_{ci}, Y_{ci})

In the first step, the users are grouped into K clusters using an unsupervised learning algorithm. K-Medoids [29] and K-Means [30] are some of the widely used clustering algorithms. For a data set, the mean represents a central value of a finite set. For calculating medoids, the dissimilarity of each point in the data set with respect to all other points is first computed. Medoids are representative objects of a data set or a cluster whose sum of dissimilarities to all other objects in that cluster is minimal. K-Means minimizes the squared error whereas K-Medoids minimizes the dissimilarity within cluster. Besides, the K-Means algorithm is sensitive to outliers since an object with an extremely large value may substantially distort the distribution of data. K-Medoids algorithm to group N users into K clusters for the deployment problem is given in Algorithm 1 where the dissimilarity index of a particular user is defined as

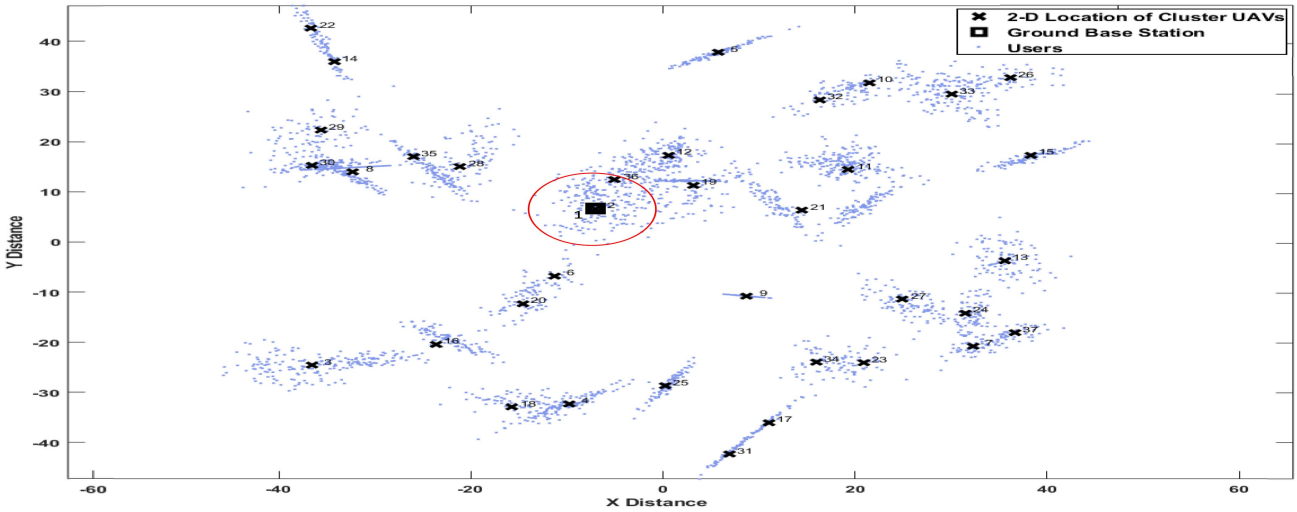

Fig. 5. Snapshot of horizontal location of cluster UAVs and location of ground base station using the proposed method.

$$V_j = \sum_{i=1}^{N} \frac{D(i,j)}{\sum_{l=1}^{N} D(i,j)}, \quad j = 1, \ldots, N \tag{4}$$

where $D(i,j)$, the distance between user i and j is defined as

$$D(i,j) = \sqrt{(X_i - X_j)^2 + (Y_i - Y_j)^2}, \quad i = 1, \ldots, N, \quad j = 1, \ldots, N \tag{5}$$

The centroids of each cluster be (X_{ci}, Y_{ci}) which would be the 2-D horizontal location coordinates of the cluster UAVs. The computational time complexity of K-Medoids clustering algorithm is $\mathbf{O}(N^2 * K * i)$, where N is the size of the data set (total number of users), K is the number of clusters, and i is the number of iterations. On the other hand, time complexity of K-Means clustering algorithm is $\mathbf{O}(N * K * i)$.

B. Location of GBS $(X_{gbs}, Y_{gbs}, h_{gbs})$

In our previous work [27], the mean location of all cluster UAVs is considered to deploy GBS. However, it is effective to find the location of GBS based on the K-Medoids algorithm. Therefore the location of GBS is determined by using the same Algorithm 1 with input as horizontal location coordinates of the cluster UAVs with K=1. One advantage of K-Medoids over K-Means is, centroid of any data set is one data point of that same set in K-Medoids while centroid of data set need not belongs to that set in K-Means. Thus, location of GBS would be horizontal location of any one of the cluster UAVs. This also gives an advantage in terms of required number of relay UAVs and reduced trajectory distance. GBS is assumed to be mounted on a truck and its height, h_{gbs} is small.

A snapshot of the output of the first two steps for a particular user distribution is shown in Fig. 5. For the considered user distribution, since K-Medoids algorithm is used, the location of GBS is same as the horizontal location of UAV_{C_i} (centroid of cluster 2). This results in less number of relay UAVs required as clusters 2 and 36 do not need relay UAVs because they are already within the coverage range of GBS.

C. Optimal Height and Transmit Power of Cluster UAVs

Once the 2-D location coordinates of cluster UAVs are computed, the next step is to find optimal height h_{ci} of each cluster UAV (UAV_{C_i}). Since the onboard power is limited, it is also necessary to optimize the transmit power (P_{ci}) of each UAV_{C_i}. However, height and required transmit power of UAV are related quantities and their relationship is described by the height and path loss relation for LoS model [31].

$$L_{LoS}(dB) = 20\ log_{10}\left(\frac{4\pi f_c d}{C}\right) + \xi_{LoS} \tag{6}$$

where L_{LoS} is the average path loss for LoS connection, ξ_{LoS} is the additional average loss of the free space propagation. ξ_{LoS} depend on the geographical environment, C is the light speed, f_c is the carrier frequency and d is the distance between the transmitter and receiver. From (6), it is evident that an increase in height results in more path loss and hence more transmit power is required for communication. Furthermore, the relation between height and probability of having LoS connection is given by [31]

$$P(LoS) = \frac{1}{1 + a \exp\left(-b\left[\frac{180}{\pi}\theta - a\right]\right)} \tag{7}$$

where $P(LoS)$ is the probability of having LoS connection, a and b are environmental dependent constant values, and θ is the angle of incidence which depends on the height of the transmitter (from Fig. 5, $\theta_i = \tan^{-1}[h/r_i]$). As height decreases, θ_i also decreases, and from (7), the probability of having LoS connection also reduces which decreases the coverage area of the UAV. Therefore, there has to be a lower bound (H_T) and upper bound ($2H_T$) to the UAV height along with the threshold limit to the probability of having LoS connection which is denoted as P_{LoS_T}. Since the increase in transmits power causes inter-UAV interference in the network, there has to an upper limit (P_T) to the transmit power (P_{ci}) of each UAV_{C_i}. This will also improve

Algorithm 2: Optimal Height and Transmit Power Estimation.

1: Use output of Algorithm 1 which are horizontal coordinates of K cluster UAVs and their corresponding M users.
2: Deploy the cluster UAVs at the horizontal location of each cluster on the ground.
3: **for** $i = 1$ to K (for each cluster) **do**
4: Arrange all the corresponding M users of i^{th} cluster in the decreasing order of distance from i^{th} cluster centroid (from 1 to M with M being farthest user).
5: **for** $j = 1$ to M (each user of i^{th} cluster) **do**
6: Solve (8) for user j and obtain h_{ci_j} and P_{ci_j}
7: **if** h_{ci_j} and P_{ci_j} satisfy constraints in (8) **then**
8: Save h_{ci_j} and P_{ci_j} as the optimal values (h_{ci}, P_{ci}) for cluster i and terminate inner for loop.
9: **end if**
10: **end for**
11: **end for**
12: Output $[h_{ci}, P_{ci}]$ for $i = 1$ to K as optimal height and optimal transmit power of i^{th} cluster respectively.

the effective utilization of limited battery power available on board.

Based on the above discussion, the following optimization problem is proposed to find the h_{ci} and P_{ci} of each UAV_{C_i}.

$$\begin{aligned}
\min_{h_{ci},P_{ci}} \quad & \beta h_{ci} + (1-\beta)P_{ci} \\
\text{s.t.} \quad & H_T \le h_{ci} < 2H_T, \quad \forall i = 1,\ldots,K \\
& 0 < P_{ci} \le P_T, \quad \forall i = 1,\ldots,K \\
& W_{ci} * log_2\left[1+\frac{P_{ci}/(d_{ij})^{\alpha}}{N(j)+I(j)}\right] \ge C_T, \forall i=1,\ldots,K, \\
& \qquad \forall j = 1,\ldots,M \\
& \frac{1}{1+a\exp\left(b\left[a-\frac{180}{\pi}\theta_{ij}\right]\right)} \ge P_{LoS_T}, \forall i = 1,\ldots,K, \\
& \qquad \forall j = 1,\ldots,M \qquad (8)
\end{aligned}$$

where β is the tradeoff factor between two optimization parameters. P_T is the power threshold of cluster UAV which is the maximum transmit power that can be used for communication. H_T is the height threshold of cluster UAV which is the minimum height that any cluster UAV can hover to. d_{ij} is the distance between the i^{th} cluster UAV and j^{th} user, C_T is the capacity threshold which is the minimum channel capacity needed to be achieved by the user, $N(j)$ is the noise power received by j^{th} user. P_{LoS_T} is the threshold probability of having LoS link between cluster UAV and users, θ_{ij} is the angle of incidence from the i^{th} cluster UAV and j^{th} user.

Here $I(j)$ is the co-channel interference power received by j^{th} user from neighboring UAVs which are using the same frequency as i^{th} cluster. This can be reduced by effectively employing the frequency reuse concept along with proper frequency planning. The frequency reuse distance is given by $D_{ci} = \sqrt{3N_c} * r_{ci}$ [28] where r_{ci} is the radius of the coverage area of i^{th} cluster, N_c is the no of clusters/cells in a group (for hexagonal shape cell pattern, no of cells in a group is N_c=7 and the number of first-tier co-channel interference cells are 6). For the scenario considered, for the size of the geographical area, and for the size of the coverage radius of each cluster, the average D_{ci} is $\approx 15\,kms$ and the effect of interference will be very minimal. The effect of interference is further investigated in the simulations for different power threshold values.

It can be observed from (8) that increase in h_{ci} may satisfy constraint 4 but may violate constraints 2 and 3. Similarly, decrease in h_{ci} may satisfy constraints 2 and 3 but may violate constraint 4. This proves that the resultant solution from (8) is optimal and convex. This can also be proved from simulation results by varying h_{ci} and observing the number of users that achieved channel capacity $\ge C_T$ (refer Fig. 12 from simulation results). Hence the convex optimization solvers [32] can be used to solve (8). If the constraints are violated then the user will not be served. If the constraints are satisfied for an arbitrary user j, then the same constraints are valid for all other users closer to the cluster center than user j. Based on this observation, Algorithm 2 is presented for optimal height and transmit power of cluster UAVs. With this, the 3-D location coordinates of cluster UAVs are found along with optimized transmit power.

IV. Trajectory Optimization of Relay UAVs

It should be noted that (also illustrated in Fig. 1 and 5) all UAV_{C_i} may not be within the coverage area of GBS. Hence, UAV_{R_i} are used to transmit data between UAV_{C_i} and GBS. The reason behind placing the GBS based on K-Medoids algorithm (Algorithm 1) is to reduce the distance traveled by UAV_{R_i}. The major cost factor for relay UAVs is the power which is limited. The combined distance traveled and distance communicated will be the crucial factor that decides the power consumed by the relay UAVs. The distance communicated depends on h_{ci} and P_{ci} which are already optimized in the previous step. Hence the key objective of trajectory optimization is to reduce the cost of UAV communication by reducing the traveling distance of a relay UAV.

To optimize the trajectory of relay UAVs, graph theory-based approaches are more suitable. In this work, the renowned cost minimization method, Dijkstra's algorithm [33] is used. Dijkstra's algorithm considers all possible routes and their cost (distances) as weights to solve the trajectory optimization problem. The inputs to this algorithm are 3-D coordinates of cluster UAVs and the location of GBS which are obtained from previous steps. For the problem in consideration, the adjacency matrix or weight matrix of Dijkstra's algorithm, $G(i,j)$ ($i = 1,\ldots,K+1$ and $j = 1,\ldots,K+1$) is proposed as below. It is to be noted that i and j are nodes in Dijkstra's algorithm which are cluster UAVs and GBS. Here, GBS is considered node 1.

$$G(i,j) = \begin{cases} 0, & i = j \\ (d_{com} * P_{com}) + (d_{mot} * P_{mot}), & i \ne j \end{cases} \qquad (9)$$

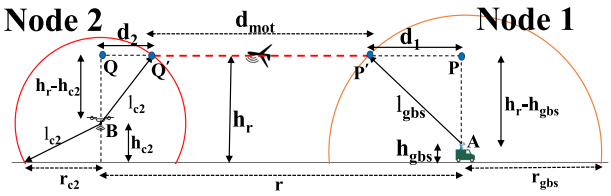

Fig. 6. Illustration of coverage area of node 1 and node 2 for computing optimal trajectory.

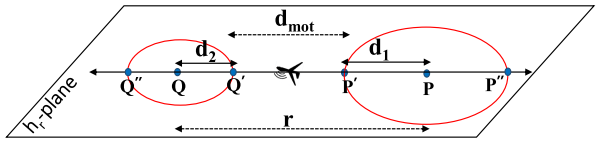

Fig. 7. 2-D cross-sectional view of coverage area of node 1 and node 2 on h_r-plane.

where P_{com} is the power required for UAV communication, P_{mot} is the power required for UAV motion (travel), d_{com} is the distance communicated, and d_{mot} is the distance traveled which are computed as follows. For relay UAVs, distance traveled refers to the total distance covered by UAV_{R_i} from node i to node j. Distance communicated is combined lengths of the communication link between UAV_{R_i} & node i and UAV_{R_i} & node j.

$$d_{com} = \begin{cases} l_{ci} + l_{gbs}, & \text{j=1} \\ l_{cj} + l_{gbs}, & \text{i=1} \\ l_{ci} + l_{cj}, & \text{otherwise} \end{cases} \tag{10}$$

$$d_{mot} = \begin{cases} 0, & d_{ij} \leq d_{com} \\ r - d_i - d_j, & d_{ij} > d_{com} \end{cases} \tag{11}$$

where d_{ij} is the distance between node i and j, l_{ci} is the length of the communication link of i^{th} node, l_{gbs} is the lengths of the communication link of GBS. r is the horizontal distance between node i and j which is illustrated in Fig. 6. Similarly from Fig. 6, d_i of a particular node (refer d_2 of node 2) is computed as

$$d_i = \sqrt{(l_{ci})^2 - (h_r - h_{ci})^2} \tag{12}$$

For calculating l_{ci}, solve channel capacity achieved by the farthest user (for example, user U1 in Fig. 2) located on the cluster edge which is given by

$$C_{ci} = W_{cu} * log_2\left(1 + \frac{P_{ci}}{(l_{ci})^{\alpha}\ N_0}\right) \tag{13}$$

where W_{cu} and P_{ci} are the bandwidth of the frequency channels used, the transmission power of the i^{th} cluster UAV respectively. And to say that the farthest user is served, $C_{ci} \geq C_T$. Therefore to find the length of the communication link of that cluster UAV, solve $C_{ci} = C_T$ which is given by,

$$l_{ci} = \left[\frac{P_{ci}}{\left(2^{\frac{C_T}{W_{cu}}} - 1\right)\ N_0}\right]^{1/\alpha} \tag{14}$$

From l_{ci}, the coverage radius of node i can be found which is given by,

$$r_{ci} = \sqrt{l_{ci}^2 - h_{ci}^2} \tag{15}$$

similarly, the length of the communication link and the coverage radius of GBS are given by

$$l_{gbs} = \left[\frac{P_{gbs}}{\left(2^{\frac{C_T}{W_{gbs}}} - 1\right)\ N_0}\right]^{1/\alpha} \tag{16}$$

$$r_{gbs} = \sqrt{l_{gbs}^2 - h_{gbs}^2} \tag{17}$$

In general, for UAVs, the Power required for propulsion (UAV motion) is much larger than the power required for communication [13], [15]. The power required for communication per distance d can be solved by (3) which is given by,

$$P_{com} = \left(2^{\frac{C_{com}}{W_{com}}} - 1\right) * d^{\alpha} * N_0 \tag{18}$$

where W_{com} and C_{com} are the bandwidth of the frequency channels used and the capacity needs to be achieved by the user located at a distance of d from the transmitter. For analysis, power required for UAV motion is considered to be 'p' times that of power required for UAV communication.

$$P_{mot} = p * P_{com} \tag{19}$$

Dijkstra's algorithm takes $G(i, j)$ as input and gives the optimal sequence of nodes that relay UAVs must transfer the information to. Since the purpose of relay UAVs is only to exchange the information between GBS and cluster UAVs, the height of all relay UAVs (h_r) is assumed to be the same and constant. To avoid collisions, $h_r > 2H_T$ whereas, from (8) $H_T \leq h_{ci} < 2H_T$.

Consider nodes 1 and 2 with centers at $A(x_A, y_A, h_A)$ and $B(x_B, y_B, h_B)$ respectively as shown in Fig. 6. Since nodes 1 and 2 are not within the communication range of each other, a relay UAV has to be used between them to relay information. The nodes here can be any combination of cluster UAV and GBS.

The relay UAVs need not travel to the nodes, but they have to be within the coverage range of the nodes. Hence the trajectory can be further optimized by properly estimating the start and end points that are within the coverage area of the nodes. Consider node 1 is GBS and node 2 is cluster UAV. In order to optimize the trajectory the start point P' and endpoint Q' (illustrated in Fig. 6) are to be computed. Since the relay UAV's height is constant (h_r), the 3-D trajectory optimization of the relay UAV is now 2-D trajectory optimization problem on Z-plane (h_r-plane) which is shown in Fig. 7.

Therefore, the intersection of h_r-plane with the coverage area of node 1 results in a circular disc of radius d_1 with center at $P(x_A, y_A, h_r)$. Hence the start point P' of the trajectory of

Algorithm 3: Optimal Trajectory Using Dijkstra's Algorithm.

1: Assign weights to communication power and travel power required [i.e. choose p in (19)].
2: **for** $i = 1$ to $K + 1$ (K cluster UAVs and 1 GBS) **do**
3: **for** $j = 1$ to $K + 1$ **do**
4: Update the weight matrix of $K + 1$ nodes in $G(i, j)$ by using (9)
5: **end for**
6: **end for**
7: **for** $i = 2$ to $K + 1$ (for each cluster) **do**
8: Solve for cost and route of i^{th} cluster using Dijkstra's algorithm with $G(i, :)$ as weight matrix, GBS as source and i^{th} cluster as destination.
9: **end for**
10: Sort out the optimal route with minimum cost from the cost and route matrix.
11: Solve for the start and end locations of optimal route by solving (20) and (21) for appropriate nodes.
12: Output start, end locations, cost, and route as optimal trajectory planning of relay UAVs

the relay UAV can be any point on the circumference of that circular disc. Similarly, the endpoint Q' can be any point on the circumference of a circular disc of radius d_2 and center $Q(x_B, y_B, h_r)$ as illustrated in Fig. 7. Here, d_1 and d_2 can be calculated using (12). d_{mot} is the shortest distance traveled by a relay UAV which can be found using (11). Now from Fig. 7, it is evident that the start point P' can be found by solving the following two equations.

$$(x - x_A)^2 + (y - y_A)^2 = d_1^2 \tag{20}$$

$$\frac{x - x_A}{x_B - x_A} = \frac{y - y_A}{y_B - y_A} \tag{21}$$

It should be noted that, solving (20) and (21) has two solutions P' and p''. In a similar way, the endpoint can be found by finding the intersection of (21) with the circle of radius d_2 and center Q which results in two solutions Q' and Q''. Since the objective is to optimize the trajectory, the pair of points [either $(P,' Q')$ or $(P,'' Q'')$] with minimal distance between them is taken as the start and end points.

Algorithm 3 illustrates Dijkstra's algorithm used for determining the optimal trajectory of relay UAVs. The algorithm finds the optimal sequence of nodes for the shortest route. The computational time complexity of Dijkstra's algorithm is $\mathbf{O}((K + 1)^2)$, where $K + 1$ denotes the number of nodes which is the sum of K cluster UAVs and one GBS. The number of relay UAVs is a user-defined quantity that depends on the resources available. The results of this section can be visualized in Fig. 8 for a particular scenario.

V. Simulation Results

The performance of the proposed algorithms is analyzed using MATLAB 2020a running on a 64-bit operating system. The computer is configured with Intel(R) Xeon(R) E-2146 G CPU @ 3.5 GHz, 8^{th} generation Intel Pentium processor, and 16 GB of DDR4 RAM. For user distribution, data points were sampled from a Gaussian mixture model derived from a uniform random distribution with a mean range of $[-40, 40]$ and a variance range of $[0, 10]$. Total N users are divided into K clusters leading to each cluster consisting of M users. The optimization tradeoff factor, β (refer to (8)) is taken as 0.5 and environmental constants are taken as $a = 3, b = 0.9$ [31] for the considered geographical scenario. The simulation parameters used are listed in Table I. Note that the number of clusters and routes are user-defined quantity and is decided based on the availability of resources such as the number of UAVs available, type of UAVs, battery capacity of UAVs etc... A particular instantiation of the user distribution is shown in Fig. 5 for illustration purposes. Also, the output of the proposed 3-D deployment for cluster UAVs is also illustrated in Fig. 5.

TABLE I
Simulation Parameters

Area of population spread	40 km x 40 km
User distribution mean range	$[-40, 40]$
User distribution variance range	$[0, 10]$
Number of cluster UAVs, K	36
Total number of users, N	3600
Number of users per cluster, M	100
Radius of coverage area of GBS, r_{gbs}	5.595 km
Transmit power of the GBS, P_{gbs}	10 W
Height of the GBS, h_{gbs}	10 m
Height of the relay UAV, h_r	1000 m
Noise Power, N_0	-7 dBm/Hz
Carrier frequency, f_c	3.5 GHz
Channel bandwidth	5 KHz
Maximum radius of coverage area of cluster UAV	3.9242 km
Channel capacity threshold, C_T	2000 bps
Power threshold of cluster UAV, P_T	5 W
Height threshold of cluster UAV, H_T	500 m
LoS probability threshold, P_{LoS_T}	0.8 (80 %)

TABLE II
Routes of Relay UAVs With Intermediate and Destination Clusters of Each Route

Route	Source	Destination cluster	clusters on route
1	1	3	$(6, 20), 16$
2	1	$(4, 18)$	$9, (23, 34), (17, 31), 25$
3	1	5	$(12, 19), (10, 32)$
4	1	$(7, 24, 37)$	$27, 13$
5	1	$(14, 22)$	$28, (8, 35), (29, 30)$
6	1	$(26, 33)$	$21, 11, 15$

Table II lists the routes of relay UAVs with intermediate and destination clusters of each route. The transmit power of relay UAV, P_{ri} of each route is considered to be the maximum of the optimized transmit power of cluster UAVs covered by that particular relay UAV in that route. The sequence of nodes to be traversed by the relay UAVs given by Dijkstra's algorithm is given in Table II for the same instantiation.

The bracketed clusters indicate that the relay UAV serves both these clusters from the same location. For example, clusters (6,20) are close to each other such that the relay UAV located between clusters 6 and 20 is within the coverage range of both clusters. The resultant optimized trajectory of relay UAVs is shown in Fig. 8.

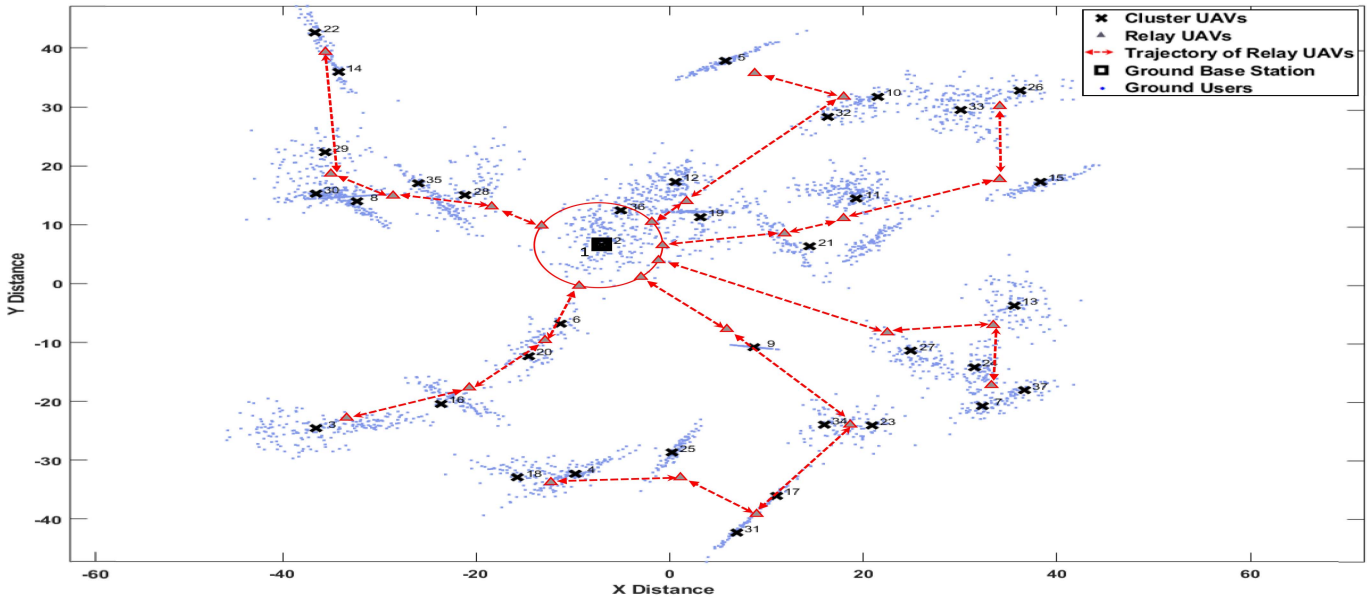

Fig. 8. Snapshot of the optimal trajectory of relay UAVs.

In order to analyze the performance of the proposed algorithm, performance metric considered is explained here. The performance of proposed algorithm is compared with uniform, GICA [23] based, k-Means [27] based 3-D deployment algorithms. It should be noted that no optimization is involved in GICA and uniform deployment algorithms. In order to analyze the clustering performance, average channel capacity achieved per each user (A) in bits per second (bps) and total number of users served (B) are considered. The average channel capacity achieved per each user (A) is given by,

$$A = \frac{Tot\_Chn\_Cap}{Total\ number\ of\ users} \tag{22}$$

where, Tot_Chn_Cap is sum of channel capacity achieved by all N users (3600 users) and is given by,

$$Tot\_Chn\_Cap = \sum_{i=1}^{K} \sum_{j=1}^{M} \left[W_{ci} * log_2 \left(1 + \frac{P_{ci}}{(d_{ij})^{\alpha}\ N_0} \right) \right] \tag{23}$$

where P_{ci} is the optimal transmit power of the i^{th} cluster UAV in watts, d_{ij} is the distance between i^{th} cluster and j^{th} user in that cluster, and N_0 is noise margin. For calculating the total number of users served (B), A user is considered to be served if the channel capacity achieved by that user is above a certain threshold.

In order to study the performance of the height-power optimization problem, optimized average transmit power per cluster (C) in watts, optimized average height of the cluster UAVs (D) in kilometers, total power saved using optimization problem (E) in watts, and percentage of power saved using optimization problem (F) are the performance metrics considered. For comparative study, the proposed K-Medoids clustering-based optimization algorithm is compared with K-Means clustering-based optimization algorithm [27]. The optimized average transmit power per cluster (C) and optimized average height of the cluster UAVs (D) are given by,

$$C = \sum_{i=1}^{K} \frac{P_{ci}}{K} \quad and \quad D = \sum_{i=1}^{K} \frac{h_{ci}}{K} \tag{24}$$

The total power saved using the optimization problem (E) is defined as the algebraic difference between the sum of transmit power used by all clusters (P_T) without optimization and the sum of optimal transmit power used by all clusters (P_{ci}) after optimization which is given by,

$$E = \sum_{i=1}^{K} [N_i \times (P_T - P_{ci})] \tag{25}$$

where N_i is the number of users served in i^{th} cluster. It is to be noted that, without optimization, cluster UAVs use power threshold P_T as transmit power and the optimization problem goal is to reduce that transmit power to less than that of power threshold ($P_{ci} \leq P_T,\ \forall i = 1, \ldots, K$). Furthermore, the percentage of power saved using the optimization problem (F) is determined as follows:

$$F\ (\%) = \frac{\sum_{i=1}^{K} [N_i \times (P_T - P_{ci})]}{\sum_{i=1}^{K} (N_i \times P_T)} \times 100 \tag{26}$$

A. *Effect of Power Threshold on Performance Metric*

Here, the power threshold (P_T) is varied from 1 to 10 watts while all other parameters are the same as in Table I and the changes in performance metric are studied.

1) for a Free Space Channel Model With LoS Connection Without Co-Channel Interference: For this channel model which is shown in Fig. 2, α is taken as 2 in the optimization problem (8). Also d_i is calculated using (1). The number of users served (B) is calculated by taking the sum of users whose channel capacity is more than 2 $kbps$. Interference $I(j)$ is considered to be zero for this case. For example, consider cluster

TABLE III
EFFECT OF POWER THRESHOLD ON AVERAGE CAPACITY PER USER (A) IN bps & NUMBER OF USERS SERVED (B) FOR FREE SPACE MODEL WITHOUT INTERFERENCE IS CONSIDERED

P_T (w)	Uniform		GICA		K-Means		K-Medoids	
	A	B	A	B	A	B	A	B
1	873	272	1987	962	2256	1156	2473	1217
2	1647	413	3358	1578	3987	1720	4073	1875
3	2581	578	4963	2013	5319	2139	5846	2354
4	3368	746	6346	2241	6576	2367	7278	2682
5	5013	1184	7531	2474	7742	2576	8541	2877
6	5348	1376	8810	2582	8938	2654	9735	2963
7	5769	1592	9594	2657	9673	2727	11067	3109
8	6271	1817	9776	2734	10173	2893	11586	3226
9	6743	2031	9872	2976	10543	3088	12127	3295
10	7932	2249	10736	3139	11248	3256	13072	3434

TABLE IV
EFFECT OF POWER THRESHOLD ON AVERAGE TRANSMIT POWER PER CLUSTER (C), AVERAGE HEIGHT OF THE CLUSTER UAV (D), TOTAL POWER SAVED USING OPTIMIZATION (E), & PERCENTAGE OF POWER SAVED USING OPTIMIZATION (F) FOR FREE SPACE MODEL

P_T (w)	K-Means				K-Medoids			
	C (w)	D (kms)	E (w)	F (%)	C (w)	D (kms)	E (w)	F (%)
1	0.937	0.5	57.53	4.83	0.946	0.5	72.46	4.73
2	1.929	0.5	102.67	4.21	1.932	0.5	138.49	5.52
3	2.917	0.587	237.48	5.48	2.905	0.575	317.43	5.52
4	3.784	0.642	579.12	6.36	3.780	0.614	603.57	6.24
5	4.726	0.726	792.15	6.17	4.731	0.699	856.33	6.48
6	5.440	0.824	983.47	7.56	5.451	0.782	1147.2	7.92
7	6.209	0.895	1872.5	8.29	6.214	0.833	2014.6	9.47
8	7.044	0.944	2453.7	10.34	7.053	0.919	2942.5	11.18
9	7.635	0.931	3142.8	12.74	7.541	0.922	3572.9	13.50
10	8.535	0.927	3963.8	13.56	8.385	0.927	4337.3	15.81

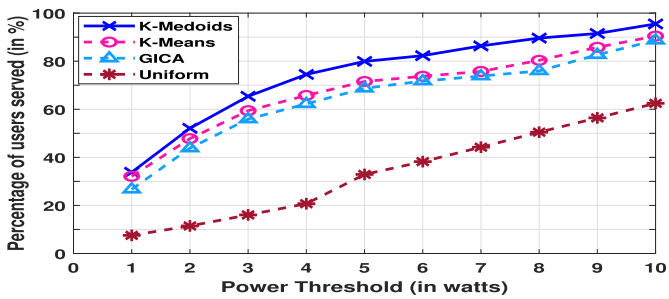

Fig. 9. Power threshold vs Percentage of users served.

25 which is having $r_{c25} = 4.3261\,kms$. Its frequency reuse distance is $D_{c25} = 19.8247kms$. Therefore from (3), the maximum interference experienced by any user from 25^{th} cluster can be $I(j) \approx 73.33\,mW$ which is minimal for the scenario considered. The results of Monte Carlo simulations are listed in Tables III and IV.

It is evident from Table III (also from Figs. 9 and 10) that as P_T increases, both average channel capacity achieved per each user (A) and the number of users served (B) are increasing because of increase in the coverage area of all clusters. It can be seen that the proposed K-Medoids based deployment algorithm outperforms the uniform, GICA, and K-Means based deployment algorithms significantly for all values of P_T in terms of performance metric.

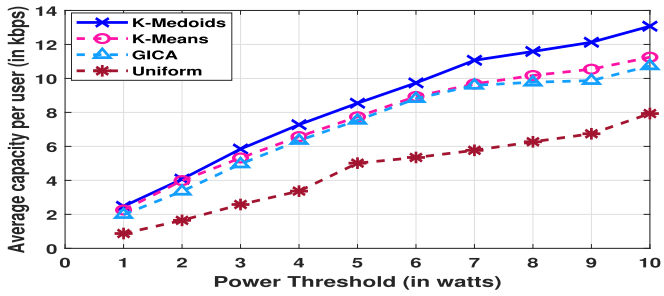

Fig. 10. Power threshold vs Average capacity per user.

TABLE V
EFFECT OF POWER THRESHOLD FOR FREE SPACE MODEL WITH AND WITHOUT INTERFERENCE CONSIDERED

P_T (w)	Without cochannel interference				With cochannel interference			
	K-Means		K-Medoids		K-Means		K-Medoids	
	A	B	A	B	A	B	A	B
1	2343	1161	2587	1198	2083	1135	2356	1176
2	3994	1683	4146	1784	3751	1674	3464	1753
3	5258	2078	5732	2325	4872	2072	4153	2267
4	6471	2254	7059	2676	5943	2239	4772	2595
5	7709	2512	8473	2881	6404	2472	5918	2762
6	8953	2643	9871	3012	7615	2587	6325	2854
7	9715	2750	11354	3153	7190	2638	7653	2961
8	10122	2886	11597	3237	8066	2743	8456	2997
9	10415	3045	12018	3279	9329	2831	9437	2965
10	11067	3237	12875	3391	9557	2968	9972	3032

It is to be noted that, columns C, D, E, and F of both K-Medoids and K-Means algorithms from the Table IV (and from all the tables henceforth) are the output of optimization problem in (8). Therefore, it is also observed that K-Medoids based optimization algorithm is saving more power compared with K-Means based optimization algorithm. This is because of the more users served by K-Medoids algorithm compared to K-Means algorithms.

2) for a Free Space Channel Model With LoS Connection With Co-Channel Interference: In this case, the effect of interference is studied for the worst-case scenario. Since frequency planning is not investigated in this work, the frequency channel information of clusters is unknown. Due to this, the distance and transmitted power of 6 co-channel interference cells are unknown to calculate co-channel interference. Because of this reason worst case scenario is considered for calculating $I(j)$ which is by considering all the other clusters which are more than frequency reuse distance apart as co-channel interference cells.

It can be observed from Table V and Fig. 11 that, the difference between number of users served (B) with and without interference is small for both K-Medoids and K-Means clustering algorithm. This reflects onto the effect of interference is minimal. Also the effect of interference is low for lower P_T values and it increases with increase in P_T. This is because the more the transmitted power of interference clusters, the more interference is. The channel capacity reduces with increasing interference. This results in less Average capacity per user (A) compared to without interference case. However, still, the performance of K-Medoids clustering algorithm is still better compared to

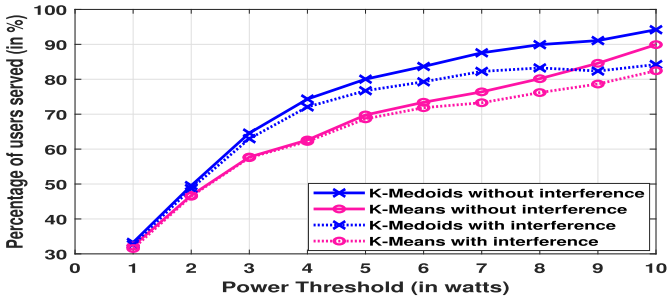

Fig. 11. Effect of interference on percentage of users served.

TABLE VI
EFFECT OF POWER THRESHOLD ON NUMBER OF USERS SERVED (B), AVERAGE TRANSMIT POWER PER CLUSTER (C), AVERAGE HEIGHT OF THE CLUSTER UAV (D), & PERCENTAGE OF POWER SAVED USING OPTIMIZATION (F) FOR HYBRID CHANNEL MODEL

P_T (w)	K-Means				K-Medoids			
	B	C (w)	D (kms)	F (%)	B	C (w)	D (kms)	F (%)
1	758	0.714	0.513	6.13	766	0.692	0.527	6.44
2	1273	1.687	0.552	5.72	1284	1.662	0.560	5.91
3	1847	2.538	0.604	5.96	1852	2.470	0.625	6.06
4	2158	3.511	0.665	6.19	2170	3.499	0.683	6.39
5	2346	4.342	0.705	6.24	2391	4.421	0.714	6.53
6	2534	5.235	0.786	7.84	2607	5.304	0.793	7.47
7	2716	6.104	0.854	8.41	2785	6.218	0.823	8.02
8	2835	6.982	0.913	9.96	2871	7.014	0.870	8.85
9	2920	7.644	0.943	11.05	2934	7.735	0.915	9.94
10	3004	8.731	0.934	12.78	3046	8.762	0.929	11.28

K-Means algorithm even for interference is considered in terms of both A and B.

3) for a Two-Ray Channel Model With Hybrid LoS and NLoS Connection Without Co-Channel Interference: For this hybrid channel model which is shown in Fig. 3, α is taken as 4 in the optimization problem (8). Also d_i is calculated using (2) where h_t refers to the height of the cluster UAV serving the users in that cluster, h_{ri} is the height of the i^{th} user. The height of the users is randomly generated in the range of 0 to 50 meters ($0 \leq h_{ri} \leq 50 meters$). Interference $I(j)$ is considered to be zero for this case also. The results of Monte Carlo simulations are listed in Table VI.

By comparing Table VI with Table III in terms of the number of users served (B) for K-Medoids and K-Means, K-Medoids clustering algorithm with hybrid channel model is outperformed by K-Medoids algorithm with free space LoS channel model. This is also true K-Means, as the K-Means hybrid model is outperformed by K-Means free space model.

Also by comparing Table VI with Table IV for lower P_T values in terms of the percentage of power saved (F), the hybrid channel model is outperforming the free space channel model. This is because, at low P_T, the number of users served is low which leads to the usage of lesser transmit power required by cluster UAVs in hybrid channel model. This resulted in more power saved than the free space LoS channel model. However, this is changed for higher power threshold values. For higher P_T, transmit power required to serve the users is increased compared with the free space channel model which leads to less power saved in comparison with the free space channel model.

TABLE VII
EFFECT OF HEIGHT THRESHOLD ON AVERAGE CAPACITY PER USER (A) IN bps & NUMBER OF USERS SERVED (B) FOR FREE SPACE MODEL

H_T (kms)	Uniform		GICA		K-Means		K-Medoids	
	A	B	A	B	A	B	A	B
0.10	6317	732	8673	1043	8939	1129	9168	1260
0.25	5691	956	8059	1962	8357	2013	8735	2158
0.50	5013	1184	7531	2474	7742	2576	8541	2877
0.75	4937	1056	7497	2487	7715	2613	8522	2924
1.00	4782	967	7318	2409	7593	2515	8437	2749
1.25	4476	912	7272	2315	7355	2416	8359	2582
1.50	4113	869	7016	2246	7146	2370	8298	2420
1.75	3759	831	6659	2057	6801	2154	8051	2216
2.00	3168	786	6186	1851	6419	2077	7608	2079
2.25	2647	637	5755	1637	6050	1896	7190	1925
2.50	2153	426	5143	1319	5476	1520	6853	1531

TABLE VIII
EFFECT OF HEIGHT THRESHOLD ON AVERAGE TRANSMIT POWER PER CLUSTER (C), AVERAGE HEIGHT OF THE CLUSTER UAV (D), TOTAL POWER SAVED USING OPTIMIZATION (E), & PERCENTAGE OF POWER SAVED USING OPTIMIZATION (F) FOR FREE SPACE MODEL

H_T (kms)	K-Means				K-Medoids			
	C (w)	D (kms)	E (w)	F (%)	C (w)	D (kms)	E (w)	F (%)
0.10	4.241	0.184	1126.74	6.35	4.219	0.189	1293.54	7.10
0.25	4.573	0.479	947.53	6.57	4.566	0.484	1028.16	7.29
0.50	4.726	0.726	792.15	6.17	4.731	0.699	856.33	6.48
0.75	4.85	0.984	681.17	5.92	4.857	0.976	784.15	6.18
1.00	4.926	1.00	568.45	4.78	4.932	1.00	636.24	5.86
1.25	4.965	1.25	426.50	3.21	4.973	1.25	542.63	4.27
1.50	4.976	1.50	289.41	1.97	4.984	1.50	387.72	3.10
1.75	4.952	1.75	236.59	2.13	4.956	1.75	296.11	2.56
2.00	4.876	2.00	197.63	2.31	4.880	2.00	235.42	2.42
2.25	4.824	2.25	168.84	2.26	4.825	2.25	192.71	2.23
2.50	4.736	2.50	124.51	2.14	4.725	2.50	162.56	2.11

B. Effect of Height Threshold on Performance Metric

Here, the height threshold (H_T) is varied from 0.1 to 2.5 kms while other parameters are kept as same as in Table I and the changes in performance metric are studied. It is to be noted that $I(j)$ is considered to be zero from here after.

1) for a Free Space Channel Model With LoS Connection: Here also in optimization problem (8), α is taken as 2 and d_i is calculated using (1). The Monte Carlo simulation results are listed in Tables VII and VIII.

At a lower height threshold, LoS probability (P_{LoS_T}) is low. This leads to coverage of fewer users. As H_T increases, P_{LoS_T} also increases which results in more user coverage. But as we keep on increasing H_T, the distance between users and cluster UAV also increases which results in serving less number of users. This is also the reason for less channel capacity achieved by users (A) with more H_T. This can be observed from from Tables VII, VIII (also from Figs. 12 and 13). It is quite evident that the K-Medoids based deployment algorithm is still noticeably better than the other three algorithms.

2) for a Two-Ray Channel Model With Hybrid LoS and NLoS Connection: In the optimization problem (8), α is taken as 4 for the two-ray hybrid channel model. d_i is calculated using (2)

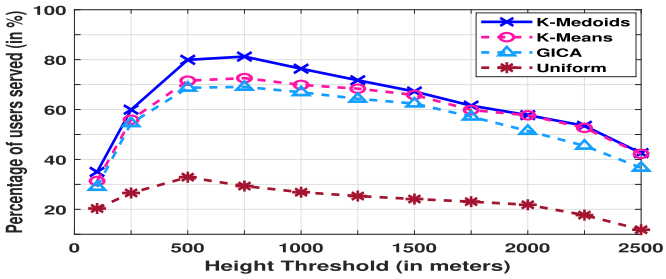

Fig. 12. Height threshold vs Percentage of users served.

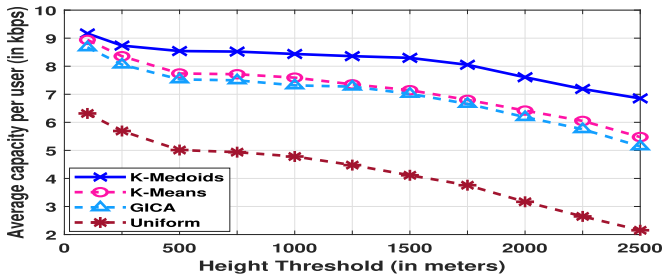

Fig. 13. Height threshold vs Average capacity per user.

TABLE IX
EFFECT OF HEIGHT THRESHOLD ON NUMBER OF USERS SERVED (B), AVERAGE TRANSMIT POWER PER CLUSTER (C), AVERAGE HEIGHT OF THE CLUSTER UAV (D), & PERCENTAGE OF POWER SAVED USING OPTIMIZATION (F) FOR HYBRID CHANNEL MODEL

H_T (kms)	K-Means				K-Medoids			
	B	C (w)	D (kms)	F (%)	B	C (w)	D (kms)	F (%)
0.10	1060	3.512	0.189	8.56	1071	3.182	0.183	9.83
0.25	1752	3.927	0.343	7.36	1805	3.834	0.462	8.51
0.50	2346	4.342	0.705	6.24	2391	4.421	0.714	6.53
0.75	2401	4.642	0.937	6.08	2450	4.752	1.024	6.37
1.00	2286	4.433	1.220	5.73	2319	4.463	1.268	6.01
1.25	2217	4.136	1.498	4.67	2298	4.028	1.521	5.74
1.50	2188	3.760	1.759	3.40	2232	3.629	1.795	5.12
1.75	2004	3.633	1.874	2.97	2143	3.579	1.934	4.63
2.00	1845	3.569	2.453	2.25	1957	3.526	2.362	3.72
2.25	1613	3.488	2.487	2.12	1676	3.484	2.431	3.25
2.50	1437	3.411	2.684	1.91	1478	3.423	2.665	2.08

where the height of the users is randomly generated in the range of 0 to 50 meters ($0 \leq h_{ri} \leq 50\, meters$). The results of Monte Carlo simulations are listed in Tables IX.

Again by comparing Table IX with Table VII and Table VIII, it is observed that the free space channel model with K-Medoids clustering algorithm is still outperforming all other three cases for all values of height threshold. However, at lower H_T, slightly more power can be saved by using the hybrid channel model with K-Medoids clustering algorithm at the cost of less number of users served.

C. Effect of Capacity Threshold on Performance Metric

Similar to the above cases, the capacity threshold (C_T) is varied from 0.5 to 5 $kbps$ with other parameters as same as on Table I, and performance is investigated. The results of Monte Carlo simulations can be observed from Tables X and XI (also from Figs. 14 and 15). Please note that only the free space channel model is considered from here after.

TABLE X
EFFECT OF CAPACITY THRESHOLD ON AVERAGE CAPACITY PER USER (A) IN bps & NUMBER OF USERS SERVED (B)

C_T (bps)	Uniform		GICA		K-Means		K-Medoids	
	A	B	A	B	A	B	A	B
500	5013	2859	7531	3056	6513	3217	6934	3343
1000	5013	2653	7531	2843	7029	3084	7714	3176
1500	5013	1856	7531	2618	7435	2893	8135	2941
2000	5013	1184	7531	2474	7742	2576	8541	2877
2500	5013	961	7531	2159	7925	2259	8740	2539
3000	5013	846	7531	1767	8201	1955	8837	2102
3500	5013	742	7531	1533	8437	1636	8954	1831
4000	5013	673	7531	1226	8660	1417	9012	1675
4500	5013	346	7531	1054	8814	1201	9073	1480
5000	5013	239	7531	735	8953	986	9157	1249

TABLE XI
EFFECT OF CAPACITY THRESHOLD ON AVERAGE TRANSMIT POWER PER CLUSTER (C), AVERAGE HEIGHT OF THE CLUSTER UAV (D), TOTAL POWER SAVED USING OPTIMIZATION (E), & PERCENTAGE OF POWER SAVED USING OPTIMIZATION (F) FOR FREE SPACE MODEL

C_T (bps)	K-Means				K-Medoids			
	C (w)	D (kms)	E (w)	F (%)	C (w)	D (kms)	E (w)	F (%)
500	3.606	0.937	4569.5	29.54	3.216	0.924	4763.7	31.69
1000	4.181	0.844	2956.1	24.47	3.838	0.847	3359.8	26.51
1500	4.517	0.751	1363.8	10.35	4.302	0.736	1637.1	11.36
2000	4.726	0.728	792.16	6.17	4.731	0.699	856.33	6.48
2500	4.764	0.701	569.09	5.96	4.805	0.679	618.59	6.13
3000	4.807	0.694	486.74	5.71	4.850	0.660	497.64	5.74
3500	4.834	0.678	429.37	5.22	4.874	0.651	424.56	5.10
4000	4.850	0.642	363.45	4.89	4.891	0.625	321.56	4.62
4500	4.866	0.632	317.51	4.13	4.904	0.607	302.68	3.81
5000	4.874	0.611	296.12	3.92	4.912	0.596	283.54	3.53

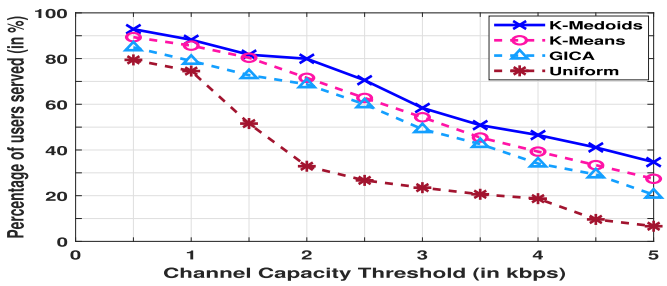

Fig. 14. Capacity threshold vs Percentage of users served.

An increase in C_T results in users far from the cluster center not achieving the required channel capacity. This results in fewer users being served (B). But the average channel capacity achieved per user (A) is the same for both uniform and GICA algorithms. This is because these two algorithms use P_T as transmit power which is the same regardless of C_T and A is calculated as the sum of channel capacity achieved by all 3600 users regardless of a user is served or not. While this is true for even K-Medoids and K-Means algorithms, the change in transmit power for change in C_T results in different A values. This can be observed in Table XI as different optimized average transmit power per cluster (C) for different C_T. Similar to

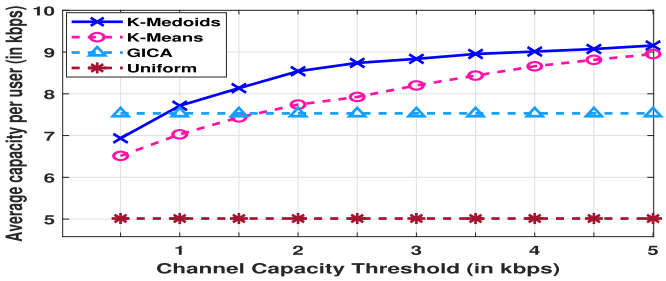

Fig. 15. Capacity threshold vs Average capacity per user.

TABLE XII
EFFECT OF POPULATION SPREAD ON AVERAGE CAPACITY PER USER (A) IN bps & NUMBER OF USERS SERVED (B)

Spread (km x km)	Uniform		GICA		K-Means		K-Medoids	
	A	B	A	B	A	B	A	B
10x10	16454	3368	20798	3589	18456	3479	19658	3491
20x20	11348	2658	15074	3297	13380	3210	14301	3263
30x30	8563	1930	9546	2946	9354	2936	10249	3051
40x40	5013	1184	7531	2474	7742	2576	8541	2877
50x50	3497	836	5177	1846	5345	2175	5863	2246
60x60	2613	507	4268	1580	4968	1756	5034	1878

TABLE XIII
EFFECT OF POPULATION SPREAD ON AVERAGE TRANSMIT POWER PER CLUSTER (C), AVERAGE HEIGHT OF THE CLUSTER UAV (D), TOTAL POWER SAVED USING OPTIMIZATION (E), & PERCENTAGE OF POWER SAVED USING OPTIMIZATION (F) FOR FREE SPACE MODEL

Spread (km x km)	K-Means				K-Medoids			
	C (w)	D (kms)	E (w)	F (%)	C (w)	D (kms)	E (w)	F (%)
10x10	2.787	0.803	6321.6	35.47	2.535	0.810	6348.7	36.02
20x20	3.561	0.786	3546.0	23.16	3.433	0.775	3469.3	22.47
30x30	4.036	0.753	1826.1	14.29	3.850	0.724	1759.1	12.46
40x40	4.726	0.726	792.15	6.17	4.731	0.699	856.33	6.48
50x50	4.937	0.701	613.93	5.88	4.835	0.646	627.56	5.94
60x60	4.893	0.688	572.47	5.22	4.795	0.624	690.82	5.83

the above cases, even here, the proposed K-Medoids based clustering algorithm performs better than all other algorithms.

D. Effect of Population Spread on Performance Metric

If population spread increases, the users are likely to be distributed far from each other as well as far from cluster center which results in fewer users to be covered (B) at lesser channel capacity achieved (A). Similarly, if the area of population spread decreases, the users are likely to be distributed close to the cluster center which results in more users being covered (B) at improved channel capacity achieved (A). Also, since users are close, a much lesser optimized average transmit power per cluster (C) is required. So here, the population spread is varied as per the Tables XII and effects are listed for Monte Carlo simulations. It is noticed that the performance of all algorithms is significantly decayed with increased population spread. But the proposed K-Medoids algorithm is still performing better than the other three algorithms.

TABLE XIV
EFFECT OF NOISE MARGIN ON AVERAGE CAPACITY PER USER (A) IN bps & NUMBER OF USERS SERVED (B)

NP (w)	Uniform		GICA		K-Means		K-Medoids	
	A	B	A	B	A	B	A	B
0.1	9357	3247	14396	3541	16152	3437	17949	3426
0.5	7853	2496	9563	3183	10231	3054	11736	3162
1	5013	1184	7531	2474	7742	2576	8541	2877
1.5	4634	960	6603	2044	6826	2207	7648	2564
2	3903	843	5945	1638	6005	1936	6796	2279
3	3356	784	4890	1479	5154	1755	5531	2008
4	2870	711	3953	1121	4278	1631	4590	1809
5	2254	633	2862	956	3350	1543	3803	1637
6	1936	405	2493	773	2733	1280	3245	1426
7	1689	276	1976	635	2321	1069	2760	1105
8	1238	192	1532	408	1976	817	2056	841
9	846	138	1339	391	1688	693	1893	736
10	575	92	1242	312	1296	547	1326	683

TABLE XV
EFFECT OF NOISE MARGIN ON AVERAGE TRANSMIT POWER PER CLUSTER (C), AVERAGE HEIGHT OF THE CLUSTER UAV (D), TOTAL POWER SAVED USING OPTIMIZATION (E), & PERCENTAGE OF POWER SAVED USING OPTIMIZATION (F) FOR FREE SPACE MODEL

NP (w)	K-Means				K-Medoids			
	C (w)	D (kms)	E (w)	F (%)	C (w)	D (kms)	E (w)	F (%)
0.1	1.744	0.851	5892.2	32.60	1.436	0.876	6359.4	35.41
0.5	3.952	0.787	2963.7	17.24	3.414	0.793	3158.3	17.85
1	4.726	0.726	792.15	6.17	4.731	0.699	856.33	6.48
1.5	4.680	0.711	637.56	5.86	4.635	0.691	772.05	5.93
2	4.654	0.709	586.04	5.37	4.618	0.687	681.19	5.46
3	4.627	0.698	531.37	4.86	4.594	0.682	566.45	5.10
4	4.607	0.685	495.42	4.49	4.581	0.676	493.20	4.74
5	4.584	0.679	440.53	3.92	4.574	0.668	436.73	4.35
6	4.564	0.674	391.10	3.51	4.568	0.654	396.39	3.96
7	4.555	0.664	348.08	2.92	4.563	0.648	354.27	3.60
8	4.548	0.650	283.55	2.70	4.557	0.643	302.52	3.22
9	4.544	0.644	209.51	2.42	4.551	0.630	248.56	2.89
10	4.536	0.640	136.56	1.93	4.546	0.621	189.01	2.05

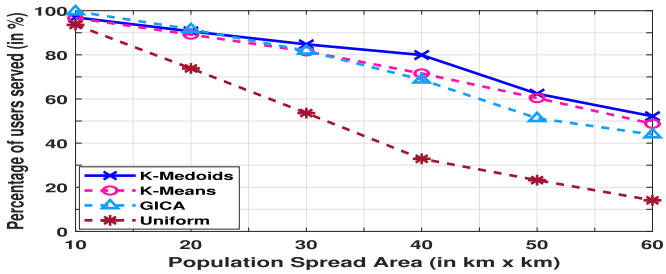

Fig. 16. Population spread vs Percentage of users served.

E. Effect of Noise Margin on Performance Metric

In all above cases, the noise margin N_0 is considered as $-7\,\mathrm{dBm/Hz}$ at a bandwidth of $5\,\mathrm{kHz}$ which is same as $1\,W$. Now, the effect of noise margin is investigated for N_0 of $0.1\,W$ to $10\,W$ ($-17\,\mathrm{dBm/Hz}$ to $3\,\mathrm{dBm/Hz}$) which is listed on Table XIV.

It is noticed that as the noise margin increases, a lesser number of users are served by all four algorithms. This is because the increase in N_0 results in decreased signal-to-noise ratio which further reduces the channel capacity achieved by

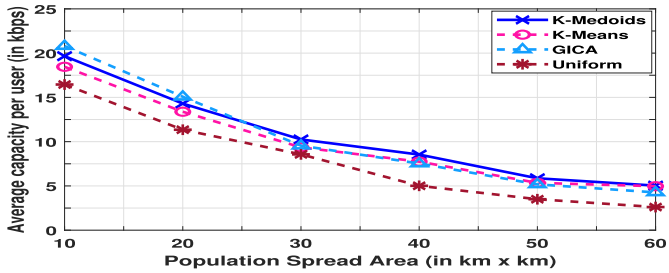

Fig. 17. Population spread vs Average capacity per user.

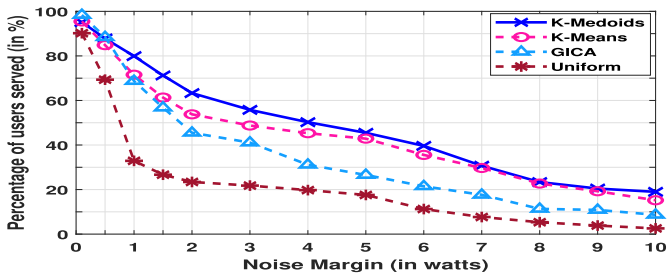

Fig. 18. Noise power vs Percentage of users served.

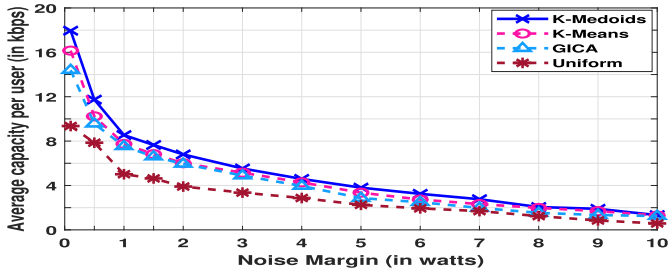

Fig. 19. Noise power vs Average capacity per user.

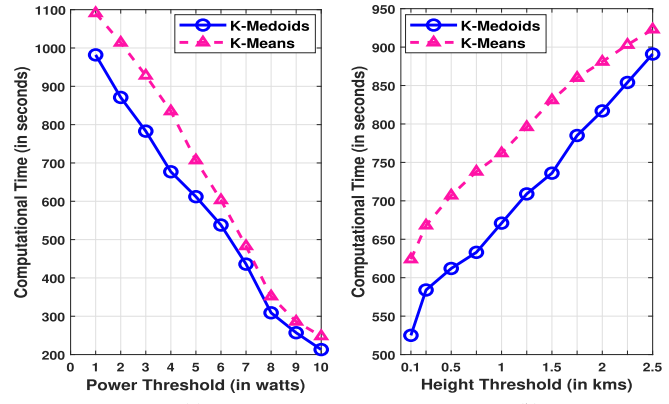

Fig. 20. Effect of power threshold and capacity threshold on the computational time taken by optimization problem.

users. However, it can be noticed from Table XIV (and from Table XV, Figs. 18, and 19) that, the proposed K-Medoids based clustering algorithm is excelling all other algorithms.

F. Effect of Optimization Parameters on Computational Time

The height-power optimization is a key algorithm and since it runs for multiple iterations for each cluster, it is a time taken process to simulate. The effect of different optimization thresholds on simulation time is investigated here and results are shown in Fig. 20. It is eminent that appropriate threshold values need to be considered for the optimization problem. The power threshold (P_T) is varied from 1 to 10 watts while the height threshold (H_T) and capacity threshold (C_T) are kept constant at 500 meters and 2 $kbps$ respectively and the computational time taken for these are plotted in Fig. 20(a). The time taken to simulate the optimization problem alone is considered as computational time here.

It is observed for lower P_T that, the computational time taken is more for both K-Medoids and K-means clustering algorithm. This is because low P_T results in the smaller coverage area of that cluster which means that the far-away users in that cluster likely to be not covered. This leaves the optimization problem to run for more iterations to evaluate the optimal P_{ci} and h_{ci}. As P_T increases, the coverage area of the cluster increases which brings about the optimization problem to run for fewer users. The effect of height threshold (H_T) is quite opposite on computational time as less H_T results in a bigger coverage area. As H_T increases, the coverage area becomes smaller. This can be observed in Fig. 20(b) for C_T of 2 $kbps$ and P_T of 5 watts. It can also be observed that K-Medoids clustering is faintly better than K-Means clustering in both Fig. 20(a) and 20(b).

G. Effect of Dijkstra's Algorithm

Since Dijkstra's algorithm is used to minimize the travel distance of a relay UAV, the performance metric of Dijkstra's algorithm are the percentage of latency reduced (F) and total power saved (G) in watts. For the simulation parameters listed in Table I, from (18), the power required for communication for 1 km distance of LoS connection, P_{com} is 0.3195 W for unit noise variance channel. From (19), the power required for the motion of UAV for 1 km distance for $p = 5$, P_{mot} is 1.5975 W (i.e. $P_{mot} = 5 * P_{com}$). It is important to notice that, Dijkstra's algorithm aims to minimize the distance traveled by relay UAVs as communication distance does not depend on relay UAVs. However, communication distance can also be minimized faintly when a single relay UAV is serving multiple cluster UAVs at a time.

The latency reduced (F) with Dijkstra's algorithm is defined as the ratio of the total distance (motion and communication distance) saved by using Dijkstra's algorithm to the total distance covered by relay UAVs without Dijkstra's algorithm. Also, the power saved (G) by Dijkstra's algorithm is defined as the difference between the sum of P_{com} and P_{mot} used by all the relay UAVs before Dijkstra's algorithm and after Dijkstra's algorithm. The effect of parameters such as P_T, H_T, and C_T on the performance of Dijkstra's algorithm is not significant enough as the distance traveled is the major factor that is important here. Therefore the effect of population spread on the performance of Dijkstra's algorithm is investigated as shown in Table XVI. It is observed that, with k-Medoids algorithm based cluster

TABLE XVI
EFFECT OF POPULATION SPREAD ON THE PERFORMANCE METRIC OF DIJKSTRA'S ALGORITHM

Spread	K-Means based clusters		K-Medoids based clusters	
(km x km)	$\mathbf{F}(\%)$	$\mathbf{G}(\mathbf{w})$	$\mathbf{F}(\%)$	$\mathbf{G}(\mathbf{w})$
$\mathbf{10 \times 10}$	22.46	2834.65	28.18	4219.06
$\mathbf{20 \times 20}$	48.94	8947.28	59.23	10916.54
$\mathbf{30 \times 30}$	59.32	17469.52	70.12	21246.08
$\mathbf{40 \times 40}$	83.29	28463.57	88.71	34899.14
$\mathbf{50 \times 50}$	88.43	42731.27	91.87	50964.33
$\mathbf{60 \times 60}$	91.81	71124.76	93.14	92344.56

UAV deployment, Dijkstra's algorithm is saving more power, reducing latency as well.

VI. CONCLUSION

3-D deployment and trajectory optimization of multiple UAVs is studied in this paper for a relay-based UAV assisted cooperative communication for emergency scenarios. K-Medoids and K-Means clustering algorithms are used for finding the horizontal location coordinates of cluster UAVs. Thereafter, optimization problem is defined to find the optimal height and optimal transmit power of each cluster UAV. Finally, Dijkstra's algorithm is used to optimize the trajectory of relay UAVs. The performance of the proposed method is validated using simulations for various possible scenarios. The effect of various parameters on the system is also studied. Simulation results show that k-Medoids based transmit power optimization of cluster UAVs is performing considerably better than k-Means based algorithm and massively outperforms uniform clustering and random clustering algorithms. Furthermore, it is observed that k-Medoids based trajectory optimization of relay UAVs saves more power and reduces extra latency than k-Means based trajectory optimization.

REFERENCES

[1] K. P. Valavanis and G. J. Vachtsevanos, *Handbook of Unmanned Aerial Vehicles*, vol. 2077, Berlin, Germany: Springer, 2015.

[2] K. Namuduri, S. Chaumette, J. H. Kim, and J. P. Sterbenz, *UAV Networks and Communications*. Cambridge, U.K.: Cambridge Univ. Press, 2017.

[3] M. Mozaffari, W. Saad, M. Bennis, Y.-H. Nam, and M. Debbah, "A tutorial on UAVs for wireless networks: Applications, challenges, and open problems," *IEEE Commun. Surv. Tut.*, vol. 21, no. 3, pp. 2334–2360, Jul.–Sep. 2019.

[4] P. V. Klaine, J. P. Nadas, R. D. Souza, and M. A. Imran, "Distributed drone base station positioning for emergency cellular networks using reinforcement learning," *Cogn. Comput.*, vol. 10, no. 5, pp. 790–804, 2018.

[5] D. N. K. Jayakody, T. D. P. Perera, A. Ghrayeb, and M. O. Hasna, "Self-energized UAV-assisted scheme for cooperative wireless relay networks," *IEEE Trans. Veh. Technol.*, vol. 69, no. 1, pp. 578–592, Jan. 2020.

[6] Y. Song, S. H. Lim, S.-W. Jeon, and S. Baek, "On cooperative achievable rates of UAV assisted cellular networks," *IEEE Trans. Veh. Technol.*, vol. 69, no. 9, pp. 9882–9895, Sep. 2020.

[7] AT&T, "Hurricane maria: Response," 2017. [Online]. Available: https://about.att.com/inside_connections_blog/hurricane_maria

[8] "Google loon," 2015. [Online]. Available: https://x.company/projects/loon/

[9] "Nasa's pathfinder," 2002, Accessed: Oct. 30, 2021. [Online]. Available: https://en.wikipedia.org/wiki/NASA_Pathfinder

[10] "Helios prototype," 1999, Accessed: Oct. 30, 2021. [Online]. Available: https://en.wikipedia.org/wiki/AeroVironment_Helios_Prototype

[11] Y. Zeng, R. Zhang, and T. J. Lim, "Throughput maximization for UAV-enabled mobile relaying systems," *IEEE Trans. Commun.*, vol. 64, no. 12, pp. 4983–4996, Dec. 2016.

[12] Y. Zeng and R. Zhang, "Energy-efficient UAV communication with trajectory optimization," *IEEE Trans. Wireless Commun.*, vol. 16, no. 6, pp. 3747–3760, Jun. 2017.

[13] C. Zhan, Y. Zeng, and R. Zhang, "Trajectory design for distributed estimation in UAV-enabled wireless sensor network," *IEEE Trans. Veh. Technol.*, vol. 67, no. 10, pp. 10155–10159, Oct. 2018.

[14] S. Yin, Y. Zhao, L. Li, and F. R. Yu, "UAV-assisted cooperative communications with power-splitting information and power transfer," *IEEE Trans. Green Commun. Netw.*, vol. 3, no. 4, pp. 1044–1057, Dec. 2019.

[15] Z. Yang, W. Xu, and M. Shikh-Bahaei, "Energy efficient UAV communication with energy harvesting," *IEEE Trans. Veh. Technol.*, vol. 69, no. 2, pp. 1913–1927, Feb. 2020.

[16] S. Yin, Y. Zhao, L. Li, and F. R. Yu, "UAV-assisted cooperative communications with time-sharing information and power transfer," *IEEE Trans. Veh. Technol.*, vol. 69, no. 2, pp. 1554–1567, Feb. 2020.

[17] P. Kumar, S. Darshi, and S. Shailendra, "Drone assisted device to device cooperative communication for critical environments," *IET Commun.*, vol. 15, no. 7, pp. 957–972, 2021.

[18] D. Zhai, H. Li, X. Tang, R. Zhang, Z. Ding, and F. R. Yu, "Height optimization and resource allocation for NOMA enhanced UAV-aided relay networks," *IEEE Trans. Commun.*, vol. 69, no. 2, pp. 962–975, Feb. 2021.

[19] M. Mozaffari, W. Saad, M. Bennis, and M. Debbah, "Efficient deployment of multiple unmanned aerial vehicles for optimal wireless coverage," *IEEE Commun. Lett.*, vol. 20, no. 8, pp. 1647–1650, Aug. 2016.

[20] J. Lyu, Y. Zeng, R. Zhang, and T. J. Lim, "Placement optimization of UAV-mounted mobile base stations," *IEEE Commun. Lett.*, vol. 21, no. 3, pp. 604–607, Mar. 2017.

[21] Q. Wu, Y. Zeng, and R. Zhang, "Joint trajectory and communication design for multi-UAV enabled wireless networks," *IEEE Trans. Wireless Commun.*, vol. 17, no. 3, pp. 2109–2121, Mar. 2018.

[22] M. Huang, L. Huang, S. Zhong, and P. Zhang, "UAV-mounted mobile base station placement via sparse recovery," *IEEE Access*, vol. 8, pp. 71775–71781, 2020.

[23] I. Mohammed, I. B. Collings, and S. V. Hanly, "Efficient multiple UAV deployment for maximizing connections with non-uniformly distributed users," in *Proc. 15th Int. Conf. Signal Process. Commun. Syst.*, 2021, pp. 1–6.

[24] Y. Zeng, J. Xu, and R. Zhang, "Energy minimization for wireless communication with rotary-wing UAV," *IEEE Trans. Wireless Commun.*, vol. 18, no. 4, pp. 2329–2345, Apr. 2019.

[25] W. Luo, Y. Shen, B. Yang, S. Wang, and X. Guan, "Joint 3-D trajectory and resource optimization in multi-UAV-enabled IoT networks with wireless power transfer," *IEEE Internet Things J.*, vol. 8, no. 10, pp. 7833–7848, May 2021.

[26] S. Chai and V. K. N. Lau, "Multi-UAV trajectory and power optimization for cached UAV wireless networks with energy and content recharging-demand driven deep learning approach," *IEEE J. Sel. Areas Commun.*, vol. 39, no. 10, pp. 3208–3224, Oct. 2021.

[27] N. L. Prasad, C. A. Ekbote, and B. Ramkumar, "Optimal deployment strategy for relay based UAV assisted cooperative communication for emergency applications," in *Proc. Nat. Conf. Commun.*, 2021, pp. 1–6.

[28] T. S. Rappaport et al., *Wireless Communications: Principles and Practice*, vol. 2. Hoboken, NJ, USA: Prentice Hall, 1996.

[29] H.-S. Park and C.-H. Jun, "A simple and fast algorithm for K-medoids clustering," *Expert Syst. Appl.*, vol. 36, no. 2, pp. 3336–3341, 2009.

[30] J. Xie and S. Jiang, "A simple and fast algorithm for global K-means clustering," in *Proc. 2nd Int. Workshop Educ. Technol. Comput. Sci.*, 2010, vol. 2, pp. 36–40.

[31] M. Mozaffari, W. Saad, M. Bennis, and M. Debbah, "Drone small cells in the clouds: Design, deployment and performance analysis," in *Proc. IEEE Glob. Commun. Conf.*, 2015, pp. 1–6.

[32] S. Boyd, S. P. Boyd, and L. Vandenberghe, *Convex Optimization*. Cambridge, U.K.: Cambridge Univ. Press, 2004.

[33] J. Zhang, J. Yu, X. Qu, and Y. Wu, "Path planning for carrier aircraft based on geometry and dijkstra's algorithm," in *Proc. 3rd IEEE Int. Conf. Control Sci. Syst. Eng.*, 2017, pp. 115–119.